Seismic performance of cold-formed steel bolted moment connections with bolting friction-slip fusing mechanism

Jun Ye[1], Seyed Mohammad Mojtabaei[2]*, Iman Hajirasouliha[3]

[1] Lecturer, Department of Architecture and Civil Engineering, University of Bath, UK

[2]* PhD candidate, Department of Civil and Structural Engineering, University of Sheffield, UK; (corresponding author). E-mail: smmojtabaei1@sheffield.ac.uk;

[3] Senior Lecturer, Department of Civil and Structural Engineering, University of Sheffield, UK

Abstract：

Typical cold-formed steel (CFS) moment-resisting connections generally have limited ductility and energy dissipation capacity due to the low local/distortional buckling resistance of thin-walled CFS elements, and therefore, may not be suitable for seismic applications. This study aims to investigate the efficiency of using bolting friction-slip fusing mechanism to improve the seismic performance of CFS bolted beam-to-column connections. To simulate the hysteretic moment–rotation behaviour and failure modes of selected connections, experimentally validated finite element models are developed using ABAQUS by taking into account the geometrical imperfections, nonlinear material properties and characteristics of the bolting fusing system. The models are then used to investigate the effects of CFS beam cross-sectional shape and classification, bolt arrangement, and slip resistance on the cyclic behaviour of the connections. It is shown that using bolting friction-slip fuse mechanism can significantly increases (up to 200%) the energy dissipation capacity, damping coefficient and ductility of the connections especially for CFS beams with thinner plates. Finally, the best design configurations are identified to improve the seismic performance of the CFS connections under strong earthquakes.

Key words: Cold-formed steel; Bolted moment connection; Cyclic behaviour; Friction-slip fusing mechanism; FE analysis

1. Introduction

Cold-formed steel (CFS) sections are produced by rolling or pressing of thin-walled steel sheets to form open cross sectional shapes at ambient temperature (cold working). In general, CFS elements can be more economical and efficient compared to their hot-rolled counterparts due to their inherent advantages such as high strength-to weight ratio, ease and speed of construction, and especially greater flexibility in manufacturing various cross-sectional profiles and sizes [1-3]. Traditionally, the use of CFS sections as main structural components has been restricted to shear walls (stud wall systems) consisting of vertical studs, diagonal braces and top and bottom tracks. The seismic behaviour of shear walls with different configurations and bracing systems has been investigated experimentally by several full-scale cyclic and monotonic tests [4-6]. While there is a consensus that most of the shear wall systems can carry lateral and vertical loads up to the drift limits required by majority of seismic codes, typical CFS shear walls may exhibit poor ductility due to the premature buckling of the stud elements [7].

In modern construction, CFS sections are increasingly being used as main structural elements in other structural systems such as moment-resisting frames in warehouses, hangars, and pitched roof industrial and agricultural buildings. Previous studies indicated that, in general, CFS bolted moment connections are capable of providing acceptable flexural strength and stiffness, and adequate deformation capacity for seismic applications [3, 8]. However, typical CFS bolted moment connections may exhibit relatively low ductility and energy dissipation capacity, especially when the width-to-thickness ratio of the CFS elements increases [9]. This limitation is a major obstacle for widespread application of CFS moment-resisting frames in multi-storey buildings in seismic regions.

Seismic design of structures normally relies on inelastic deformations through hysteretic behaviour, leading to damage and permanent deformation of structural elements, and

2

hence high repair costs, following a strong earthquake event. In steel construction, using friction-slip fusing mechanism is known as an alternative seismic design approach, implemented to absorb the energy of the earthquake and consequently reduce and control the damage to the structural elements [10] . In general, development of plasticity in the connection zone of CFS moment-resisting frames cannot be easily achieved due to the higher vulnerability of thin-walled elements (i.e. with large width-to-thickness ratio) to local/distortional buckling compared to their hot-rolled counterparts [9]. Therefore, accommodating friction-slip fusing mechanism in CFS bolted moment connections to dissipate the earthquake input energy can provide a practical solution to improve the seismic performance of CFS moment-resisting frames. In practice, friction-slip fusing mechanism can be easily activated in bolted moment connection by providing appropriate bolt tightening and detailing [10], which is presented schematically in Fig. 1.
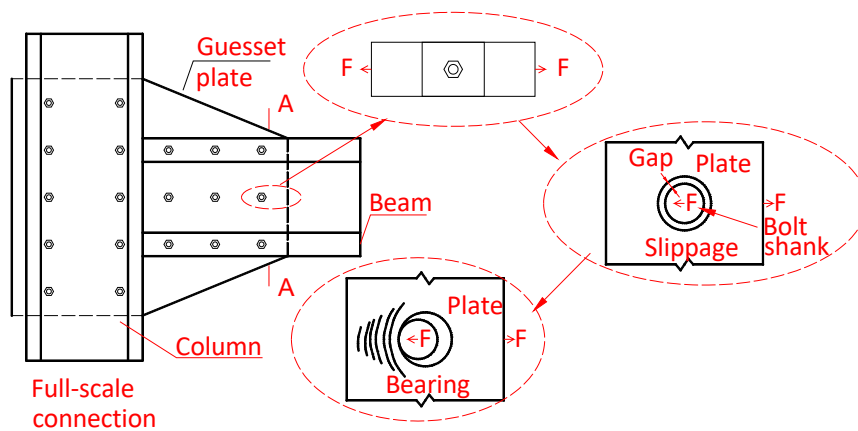
Fig. 1: Slippage and bearing behaviour of a single bolt against steel plate in a CFS bolted moment connection

The behaviour of beam-to-column CFS bolted moment-resisting connections with gusset plates has been investigated experimentally and numerically under monotonic and cyclic loading conditions [10-16]. It was found that the typical behaviour of CFS bolted connections can be characterized by a linear deformation phase followed by a slip range, a strength hardening response due to the bearing action of bolt shank against the steel sheet and

finally a strength degradation phase caused by the local buckling of the connected CFS elements. It was also demonstrated that, though CFS moment-resisting connections usually exhibit a semi-rigid behaviour, they can generally provide enough stiffness and moment resistance for low to medium rise moment frames [15]. In another study, Lim et al. [3] examined experimentally the ultimate strength of bolted moment-connections for CFS channel-sections. The tested specimens included apex and eaves connections, and it was concluded that the connections exhibit a semi-rigid behaviour due to bolt-hole elongation in the thin-walled steel sheet. Analytical work by Lim et al. [8] indicated that bolt-group sizes in CFS connections can also have a significant impact on the bending capacity of the connected sections. Based on the above studies, it can be concluded that the ductility and energy dissipation capacity of CFS bolted connections depend mainly on the following four factors: (a) bolt distribution and bolt tightening (bolt slippage); (b) material yielding and bearing around the bolt holes; (c) yielding lines resulting from the buckling of the CFS cross-sectional plates; and (d) cross-sectional shapes of the CFS beam elements. The effects of these factors will be investigated in this study. This paper aims to develop more efficient design configurations for CFS bolted moment connections with bolting friction-slip fusing mechanism to improve their ductility and energy dissipation capacity, and therefore, facilitate their application in earthquake resistant frames. Detailed GMNIA FE models are developed by taking into account material nonlinearity and initial geometrical imperfections. To model the friction-slip fusing mechanism, equivalent connector elements are used to simulate the bearing behaviour of a single bolt against CFS plate as well as the slip action of the bolts. The detailed FE models are then verified against experimental results of CFS bolted connections under cyclic loading using test data by Sabbagh et al. [10]. Subsequently, an extensive parametric study is conducted to investigate the effects of a wide range of design parameters including cross-sectional shape and classification, slip resistance, and bolt

arrangement on the behaviour of the connections. The results are then used to identify the most efficient design solutions for CFS bolted moment connections with fuse mechanism.

2. Experimentally Validate FE models

The results of previous studies have demonstrated the adequacy of detailed Finite Element (FE) models to predict the behaviour of CFS connections under monotonic [17, 18] and cyclic loading [19]. This section describes the details of the FE models developed in this study, including the model proposed for simulating bolting friction-slip fusing mechanism in a connection assembly.

2.1 Element type, loading and boundary conditions

The general-purpose S8R element (8-noded quadrilateral shell element with reduced integration) in ABAQUS [20] element library is adopted to model the CFS connection components. Following a comprehensive mesh sensitivity study, the mesh size 20×20 mm is used as it could provide a balance between accuracy and computational efficiency. The boundary conditions are applied according to the details of the test set-up presented by Sabbagh et al. [10], as shown in Fig. 2. The translational degrees of freedom U_X and U_Y on top face of the back-to-back channel column are restrained, while the bottom of the column is considered to be pinned. Since the back-to-back beam was assembled with bolts and filler plates in the experimental tests, the web lines are connected together in the U_X, U_Y and U_Z direction using the "Tie" constraint in ABAQUS [20]. Lateral bracing in the X direction is imposed at the locations of lateral frames used in the experiments to prevent lateral torsional buckling of the beam element [10] (see Fig. 2). While it was previously shown that the deformation of panel zone can also contribute to the rotational response of bolted moment connections [21, 22], due to the use of a thicker cross-section and column stiffeners in this study, it is assumed that the panel zone remains elastic during cyclic loading. This is consistent with the experimental results reported by Sabbagh et al. [10].
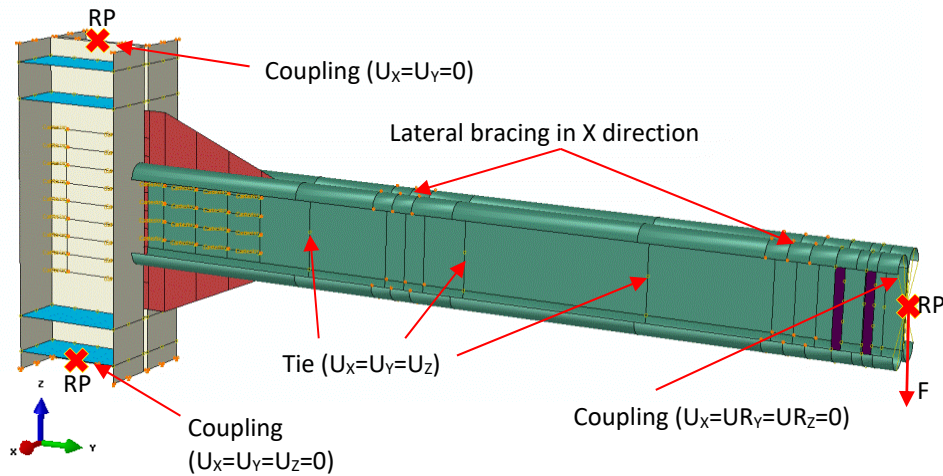
Fig. 2: Boundary conditions of the FE model for beam-column connection

To apply the external cyclic load, the nodes of the beam end section are coupled to the reference point placed on the cross-sectional centroid. A tip displacement corresponding to rotation of the connection is applied at the reference point. The AISC 341-16 [23] cyclic loading regime used in the reference experimental tests [10] is adopted as shown in Fig. 3. The displacement control nonlinear FE analyses are conducted using Static General Analysis available in ABAQUS [20] library.
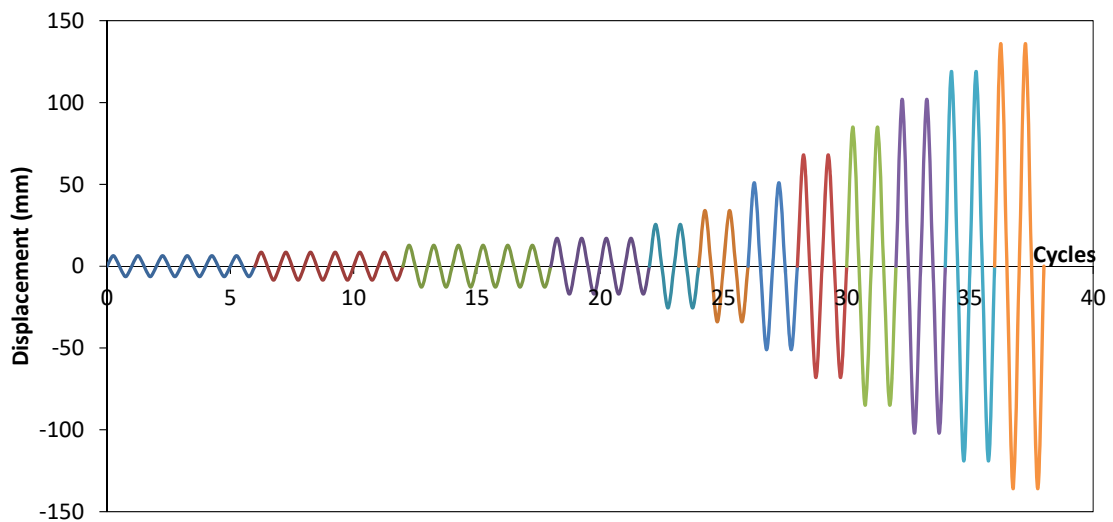
Fig. 3: Cyclic loading regime for the reference test [10] and numerical study

2.2 Material properties

The stress-strain behaviour of CFS plate is simulated using the constitutive model suggested by Haidarali and Nethercot [24]. This stress-strain relationship consists of a Ramberg-Osgood equation up to the 0.2% proof stress, followed by a straight line with a slope of $E/100$ (E is the elastic modulus) as shown below:

$$\varepsilon = \frac{\sigma}{E} + 0.002\left(\frac{\sigma}{\sigma_{0.2}}\right)^n \qquad for\ \sigma \leq \sigma_{0.2}$$

$$\varepsilon = \varepsilon_{0.2} + \frac{100(\sigma - \sigma_{0.2})}{E} \qquad for\ \sigma \geq \sigma_{0.2}$$

(1)

where $\sigma_{0.2}$ is the 0.2% proof stress, $\varepsilon_{0.2}$ is the strain corresponding to the 0.2% proof stress and n is a parameter determining the roundness of the stress-strain curve. Based on the results of coupon tests conducted by Sabbagh et al. [10], the parameter n is taken as 10, $\sigma_{0.2} = 310 MPa$, $E = 210 GPa$ and the ultimate strain is considered to be 0.08. Fig. 4 demonstrates the good agreement between the stress-strain curve from the coupon tests [10] and the material model used in this study.
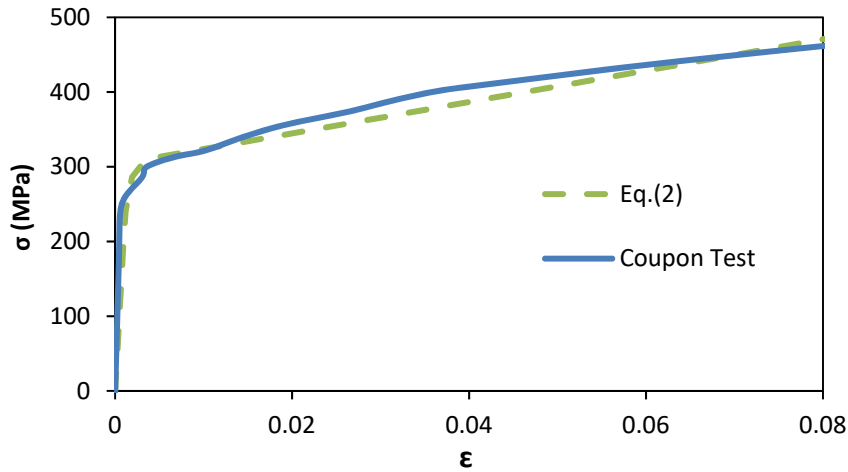
Fig. 4: Stress-strain curve used in the FE model.

2.3 Imperfection

As mentioned before, no global buckling (lateral-torsional buckling) was observed in the tested reference beam [10] due to the lateral bracing system used in the test setup. Therefore, either a local or a distortional imperfection is incorporated into the FE model, depending on which mode has the lower critical buckling resistance. The imperfection magnitude for the thickness of steel sheet (t) less than 3mm is taken as $0.34t$ and $0.94t$ for the local and distortional imperfections, respectively, based on the work conducted by Schafer and Peköz [25]. For steel sheet thickness (t) larger than $3mm$, the imperfection magnitude is considered to be $0.3t\lambda_s$ as suggested by Walker [26], where λ_s is the cross-sectional slenderness. The cross-sectional shape of the imperfection is generated by using an eigenvalue buckling analysis in ABAQUS. The first buckling mode of the CFS connection is then used to find the general shape of the local and distortional imperfections. In the case of monotonic load, a tip displacement in the Z direction is used to conduct the eigenvalue buckling analysis, which results in a unsymmetrical mode for including imperfection (see Fig. 5 (a)). However, in the case of cyclic loading, there is a need to generate a symmetrical imperfection mode (see Fig. 5 (b)). To generate this, eigenvalue buckling analysis is performed on the both +Z and -Z directions, and the mixture of the first buckling mode shapes is incorporated as an initial state of the CFS bolted moment connection.

Fig. 5: First buckling mode shape in the cases of: (a) monotonic load (b) cyclic load.

2.4 bolt modelling

In this study, a simplified connection element based to the concept of "component method" [27] is adopted to simulate the CFS connection behaviour. The slippage behaviour of the bolted connections depends mainly on the distribution of initial friction forces, which in return rely on the bolt pretension force P_b for a given applied torque and friction coefficient μ of the contact surfaces. Therefore, the bolt slip resistance F_{slip} can be expressed as [15] :

$$F_{slip} = \mu \cdot P_b \cdot n_b \tag{2}$$

where μ is the mean frictional coefficient given as 0.19 for galvanised steel surfaces [28], and n_b is the number of slip planes.

The point-based "Fastener" using a two-layer fastener configuration found in ABAQUS library [20] is employed to model individual bolts (see Fig. 6). Each layer is connected to the CFS beam and gusset plate using the connector element to define the interaction properties between the layers. To model the connector element, a "physical radius" r is defined to represent the bolt shank radius and simulate the interaction between the bolt and the nodes at the bolt-hole perimeter. This reduces the stress concentration around the nodes at the bolt positions and, hence, improves the convergence of the cyclic nonlinear analysis.
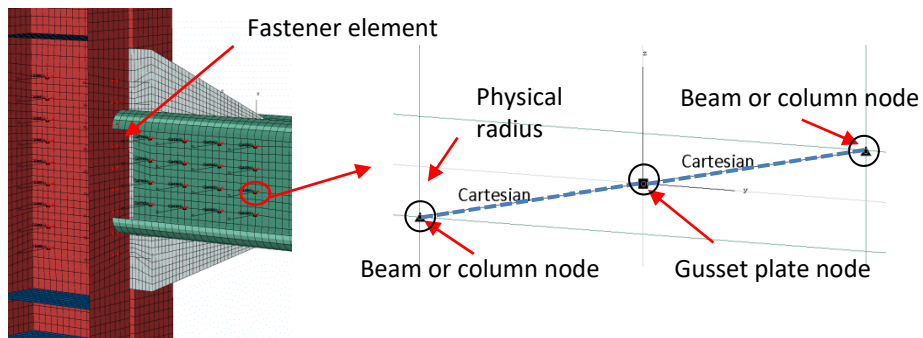
Fig. 6: FE model of the beam-column connection with fastener definition

As shown in Fig. 7 (a), each fastener point is connected to the CFS steel plates using a connector element that couples the displacement and rotation of each fastener point to the average displacement and rotation of the nearby nodes. The friction-slip fusing behaviour is assigned to the connector element using "Cartesian" with 3 translational degrees of freedom, characterised by a parallel combination of "Elasticity", "Friction" and "Stop" behaviours, as shown in Fig. 7 (b). To model "Elasticity" characteristic, a rigid behaviour is assigned to the local coordinate system corresponding to the shear deformation of the bolts. The friction coefficient μ and internal contact force P_b in Eq. (2) are used to model "Friction" behaviour. The "Stop" behaviour is thereby defined to limit the range of slip movement within the bolt-hole clearance (typically ±1mm for standard bolts by assuming that the bolt shanks are centrally positioned). The connector behaviour is schematically presented in Fig. 7 (c).
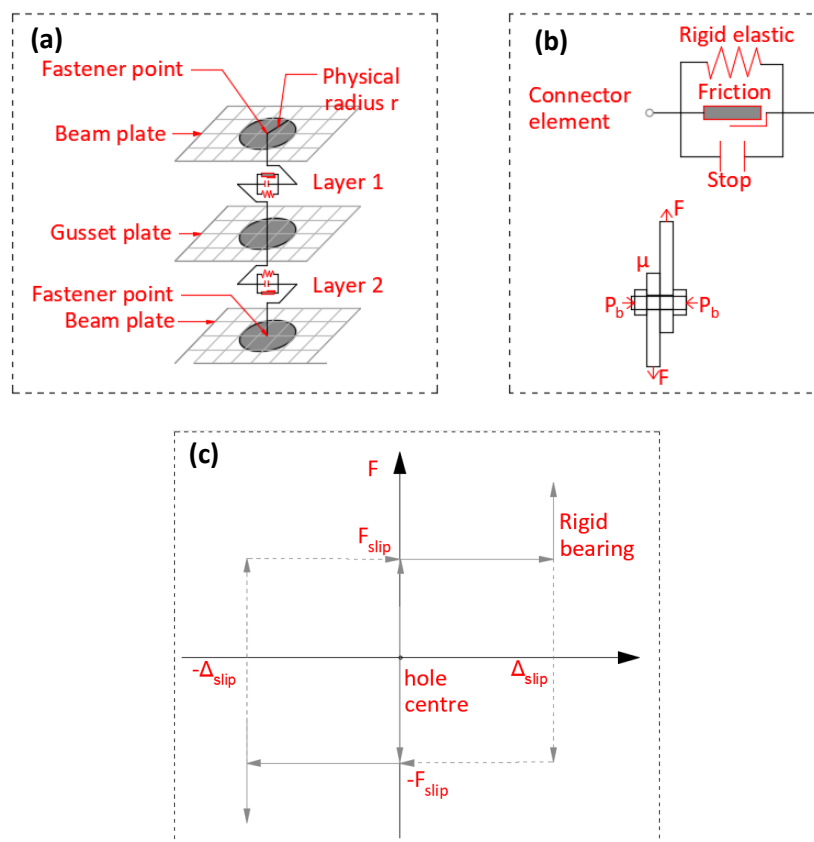
Fig. 7: Single bolt modelling in ABAQUS: (a) definition of fastener; (b) components defined in a connector section; and (c) slip-bearing relationship defined in a connector section

10

Based on the above discussion, the connector behaviour is characterised as follows:

(a) The connector is reasonably assumed to be rigid up to the slip resistance F_{slip} before the slippage of bolts (fusing mechanism) is activated. It should be noted that no slippage can be captured in FE analysis if the internal bolt force is smaller than the critical slip resistance.

(b) Connector shear force is gradually developed and overcomes frictional resistance (F_{slip}), and subsequently relative slippage between the two plates in each layer of the CFS connection starts to happen (see Fig. 7 (a)). The slippage will stop when the bolt shank is in contact with the hole perimeter surface.

(c) The bearing stiffness is infinite when the relative displacement between two fastener points is larger than Δ_{slip}.

2.5 Validation of FE models

Fig. 8 shows the moment-rotation hysteresis behaviour of the CFS connection test B2 [29], which is used to validate the developed detailed FE models. This connection is mobilised with a friction-slip fusing mechanism, which activates the bolt slippage before the buckling of CFS beam profile. Based on Eq. (2), the pretension force in the bolts is directly related to the applied torque. In the reference experimental test, the friction force between the steel plates was provided through pre-tensioning the bolts with a torque of 240 *N·m* [29]. The torque was controlled by using a torque wrench and the preloading-torque relationship was established by using a pretension measuring machine [29].

The simplified bolt model in Fig. 7 is used for modelling of the bolts, and the physical radius is defined in accordance with the bolt shank radius equal to 9 mm [29]. To partially account for the effect of bolt elongation of the plate holes, the range of slippage of the stop element in Fig. 7 is increased from ±1*mm* to ±2*mm* in the first lines of the bolts [10]. The experimental measurements and FE responses subjected to both monotonic and cyclic loading are presented in terms of moment-rotation (*M-Ө*) hysteretic curves in Fig. 8. For

better comparison, Fig. 9 also compares the failure shape of the modelled connection under cyclic loads with the experimental observations. Generally, the numerical simulation under cyclic load is in a very good agreement with the corresponding experimental results. However, the *M-θ* curve subjected to monotonic load shows less strength degradation than the response under cyclic load. This is due to the cyclic deterioration effects which cannot be captured in the case of monotonic loading. It is worth noting that reduced slip resistance was observed after a number of cycles in the experiment [10]. This is mainly due to the fact that the high torque applied in the assembling process affects the contact surface between the plates after a number of loading cycles and the new slippage force will be then stabilised. The slippage resistance corresponding to the normal surface contact condition defined in Eq. (2) proved to be reasonable in the numerical validation of FE modelling against tested results in this study. It is shown in Fig. 9 that the developed numerical model can capture successfully the shape and the position of local/distortional buckling in the CFS beam as well as bolting friction-slip fusing mechanism. These results validate the modelling approach used in this study.

(a)   (b)
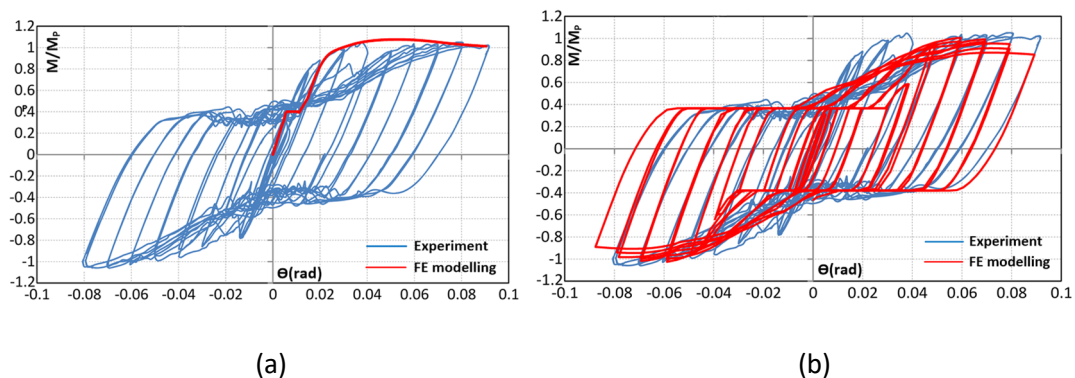
Fig. 8: Comparison between tested and analysed moment-rotation curves of connection B2 (tested by Bagheri et al. [10]): (a) monotonic load and (b) cyclic load
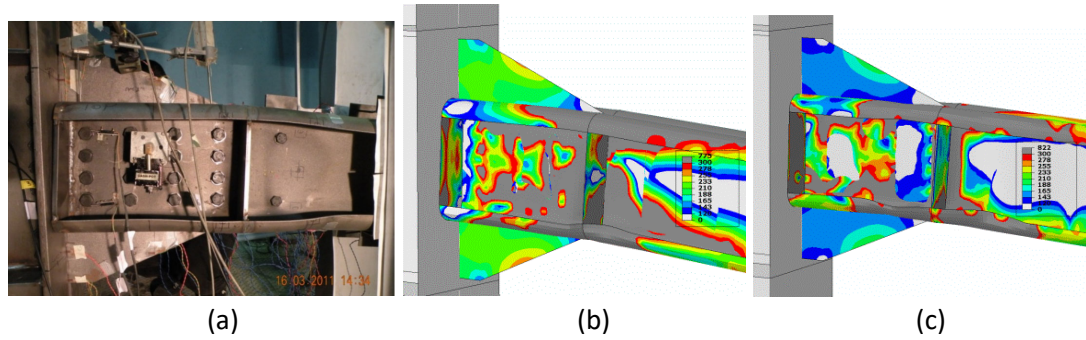
Fig. 9: Comparison between tested and analysed buckled shape of connection B2: (a) experimental cyclic load (adopted from [29]), (b) FE monotonic load, and (c) FE cyclic load

3. General response of connections with and without friction-slip fusing mechanism

CFS bolted moment connections with bolting friction-slip fusing mechanism can be considered as friction dampers, which can reduce damage in structural elements by absorbing a part of earthquake input energy and also decrease maximum stresses in connection zones by providing a fusing mechanism. To show the efficiency of the proposed system, the flexural deformation and the von-Mises stress distribution of the connections with and without bolting friction-slip fusing mechanism are extracted from FE analysis and compared in Fig. 10. While the details of the FE models for both types of connections are similar (see Section 2), bolt slippage is prevented in the connections with no friction-slip fuse mechanism by using very high pretension force values [30]. The results in Fig. 10 confirm that using the proposed fusing mechanism can significantly reduce the stress concentrations in the connection zone.

In general, the flexural behaviours of a typical CFS bolted moment connection and the one which friction-slip mechanism is mobilised through slippage of the bolts can be distinguished in different phases as shown Fig. 11. The first phase (O-A) occurs during initial loading of the connection corresponding to the elastic performance of the connection. During this phase, the bearing action of the bolts occurs for both types of connection. However, in the connection with friction-slip fuse the bearing action is interrupted at slip

moment M_{slip} (point A), which corresponds to the beginning of bolts slippage phase. The total slippage (θ_b) in the connection can be determined based on the summation of bolt holes clearance and elongation. It will be discussed in section 4 that the slip moment (M_{slip}) and bolt clearance are the key parameters which affect the energy absorbing capability of friction-slip fusing systems.

As can be seen in Fig. 11, point B corresponds to the position that the bearing action of the bolts is re-activated. Points C and C' show the peak moments (M_p) of the CFS bolted moment connections with and without bolting fusing mechanism, respectively. In the final stage, there is a sudden loss of strength for both connections due to local buckling of the beam element. In this study, it was assumed that the ultimate moment of both connections (M_u) is reached at 20% drop from peak moment (points D and D' for connections with and without friction-slip fusing mechanism, respectively).
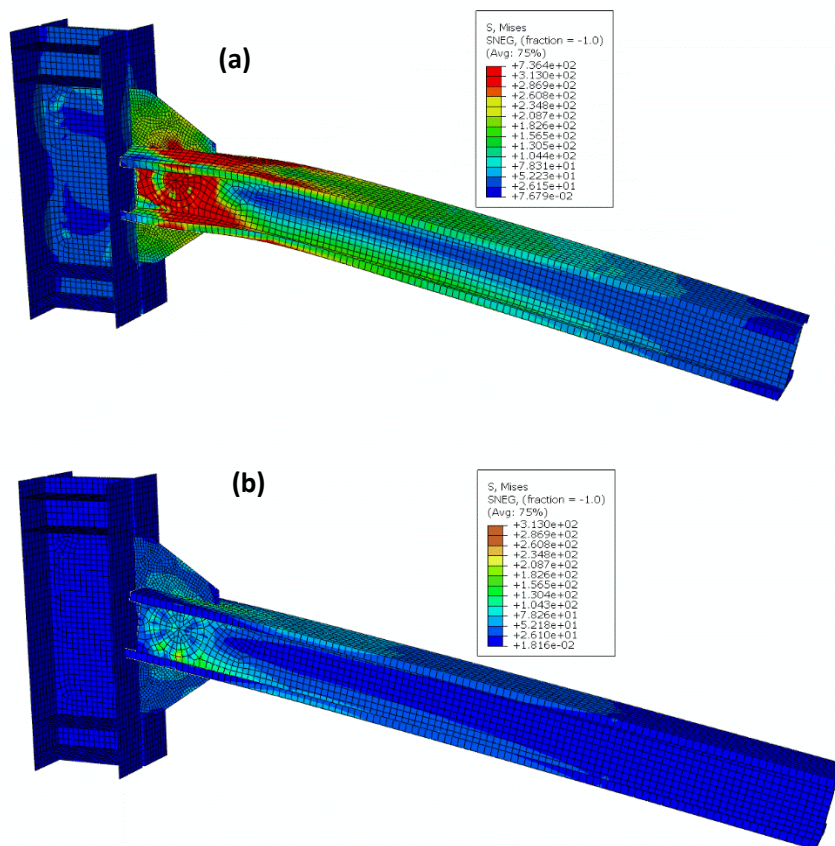
Fig. 10: Von-Mises stress distribution and coressponsing damage in the (a) normal, and (b) mobilised friction-slip connections
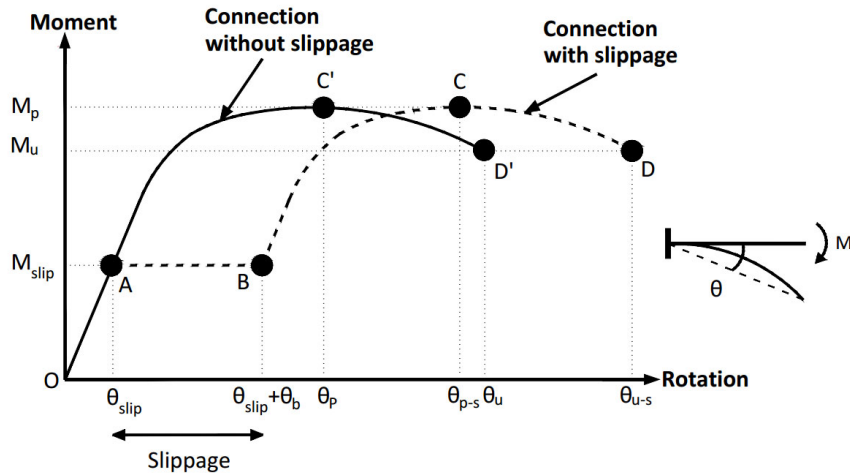
Fig. 11: Moment-rotation relationships of CFS connections with and without bolting fusing mechanism

Fig. 12 compares the cyclic hysteretic performance of the CFS bolted moment connection without and with friction-slip fuse mechanism under cyclic loading regime shown in Fig. 3. The results indicate that, similar to monotonic behaviour, using friction-slip fusing mechanism provides a horizontal shift in each cycle of hysteretic moment-rotation curve while the peak and ultimate moments are not considerably affected. This will be discussed in more detail in the following sections.
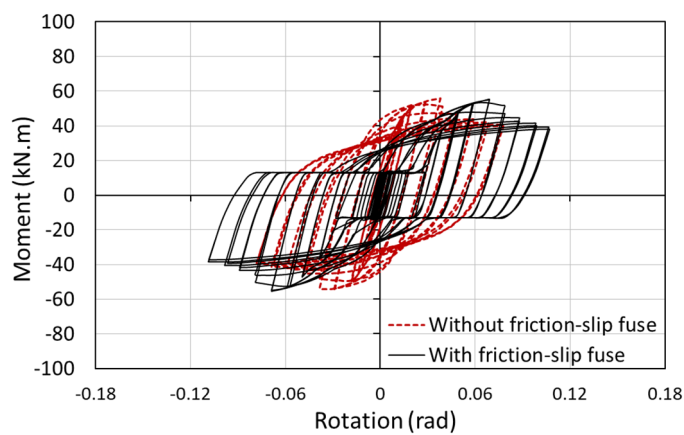
Fig. 12: Example of comparison between cyclic hysteretic performance of the CFS bolted moment connection without and with friction-slip fuse mechanism

4. Key design parameters

The main design parameters examined are beam cross-sectional shape, plate thickness (or cross-sectional slenderness), bolt configuration and bolt slip load resistance. Considering the capabilities of the cold-rolling and press-braking processes to provide cross sections with intermediate stiffeners or folded plates, four different geometries including flat, stiffened, folded and curved shaped channel cross-sections are selected for the parametric study, as shown in Fig. 13. For each cross-section, four different plate thicknesses of 1, 2, 4, 6 *mm* are used. The selected cross-sections have the same total plate width, and therefore, use the same amount of structural material. Moreover, to investigate the effect of different flange shapes, all cross-sections are designed to have a similar web slenderness ratio. It should be mentioned that the curved-flange cross-section in this study is less practical and is mainly used for comparison purposes and verification of analytical models with the reference experimental results [10]. It should be noted that thin walled sections with curved or folded-flange cross sections may be sensitive to crippling due to support transvers actions from joints and purlins, which should be considered in the design process of these elements. Since bolt configuration can also affect the stress field distribution of bolted moment connections [8], three types of bolt configurations including circle, diamond and square shapes are selected, as shown in Fig. 14. To increase the efficiency of the proposed connection, the number of bolts and their arrangement were also optimised in this study. As a result, the number of required bolts was reduced from 16 in the reference experimental tests [10] to 9 bolts. It is worth mentioning that in common construction practice the circular bolt arrangement may be less practical compared to square and diamond arrangements, however, in this study it is investigated for comparison purposes.

Flat-flange	Stiffened-flange	Curved-flange	Folded-flange
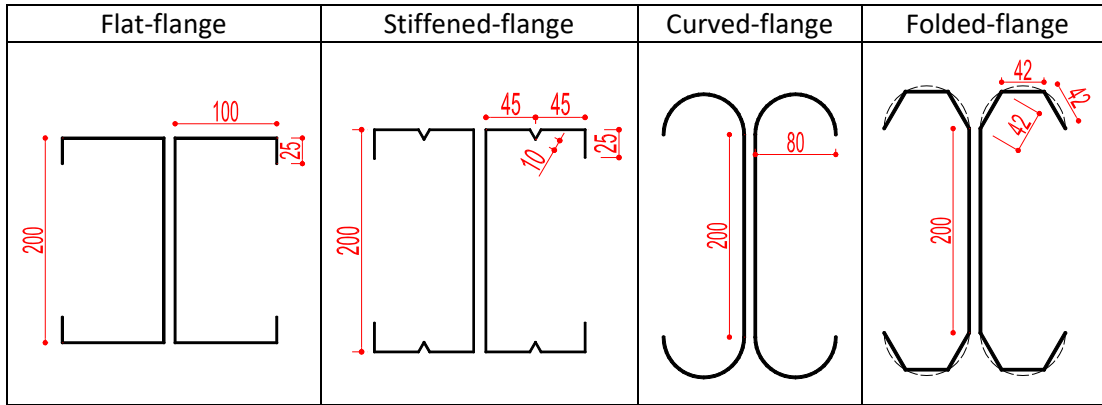
Fig. 13: Details of the back-to-back beam sectional dimensions with L=2000 mm

Bolt configuration-1	Bolt configuration-2	Bolt configuration-3
Square	Circle	Diamond
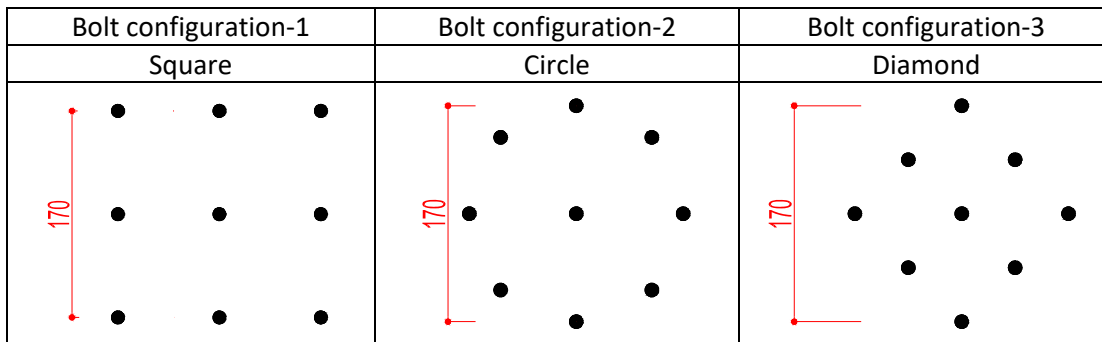
Fig. 14: Different bolt configurations

4.1 Cross-sectional classification

Eurocode 3 (EC3) categorizes cross-sections into four different classes (1, 2, 3 and 4) according to their susceptibility to local buckling. This classification can be conceptually conducted by using moment-rotation behaviour (M-θ) of the cross-section, where M_y, M_p and M_u represent yield moment, plastic moment and peak moment capacity, respectively (see Fig. 15). Class 4 cross-sections generally experience local buckling before attaining the yield moment capacity ($M_u<M_y$). In class 3 cross-sections, the stress in the extreme compression fibre reaches the yield strength, but local buckling prevents the development of the plastic moment resistance ($M_y <M_u<M_p$). Class 2 represents cross-sections that reach to their plastic moment capacity, but their ultimate plastic rotation is limited by occurrence of local plastic buckling of compression part ($M_p<M_u$). Class 1 cross-sections can develop their full plastic moment capacity with adequate plastic rotation ($M_p<M_u$). According to the

FE results, in this study all cross sectional shapes with 1, 2, 4 and 6 mm plate thickness are classified as class 4, 3, 2 and 1, respectively [30].
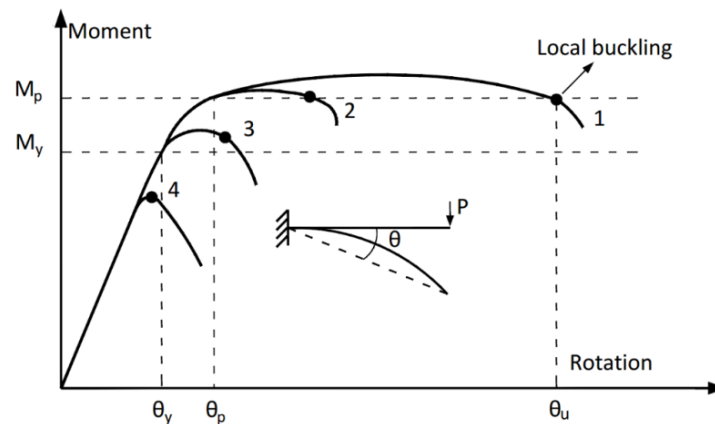
Fig. 15: EC3 cross-sectional classification definition

4.2 Effect of various bolt slip resistance

To evaluate the effect of using various bolt slip resistance on the global moment-rotation behaviour of the connections, a range of bolt pretensions are applied on the connections with the beam flat-flange class 1 (t=6mm). The slip resistance design values are selected to be at least equal to the allowable slip resistance determined according to ASTM A325 [31] using the following equation:

$$R_n = 1.13 \mu N_b T_m \tag{3}$$

where R_n is slip resistance of the connection, μ is the frictional coefficient, N_b is the number of bolts, and T_m is minimum bolt pretension. Monotonic analyses are then carried out on the connections with three different bolts pretensions using "Static General" analysis available in ABAQUS library [20]. Bolt pretensions are selected to be: T_m=90 kN which activates the bolt slippage while the CFS beam is still in the elastic behaviour range, T_m=270 kN which activates the slippage of the bolts when CFS is in its inelastic behaviour range, and fully clamped beam (no friction-slip fuse). As shown in Fig. 16, the adopted fuse mechanism generally generates a horizontal shift in the moment-rotation curve while the global behaviour of the connection is very similar to the no slippage connection. It should be noted

that, depending on bolt configuration, the behaviour of the connection with friction-slip fuse in inelastic range (especially after buckling) may be slightly different compared to the connection with no friction-slip fuse. It can be also seen in Fig. 16 that changing the value of the bolt pretension force can shift the starting point of slippage in moment-rotation curve while performance of the connection in both elastic and inelastic stages remains unchanged. It is worth noting that while the dominant failure mode in CFS bolted moment connection is local buckling of the beam close to bolt group, accommodating bolting friction-slip fusing mechanism in the connection using different bolt-pretension force and bolt configurations did not change the failure mode. Consequently, activation of friction-slip action in CFS bolted moment connections provides a means to adjust the global behaviour of the connection, especially when higher class beam sections (thicker elements) are utilised. Friction-slip fuse and its effects on maximum moment capacity, energy dissipation and damping coefficient will be discussed in Section 5 by using the results of cyclic analyses on the connections.
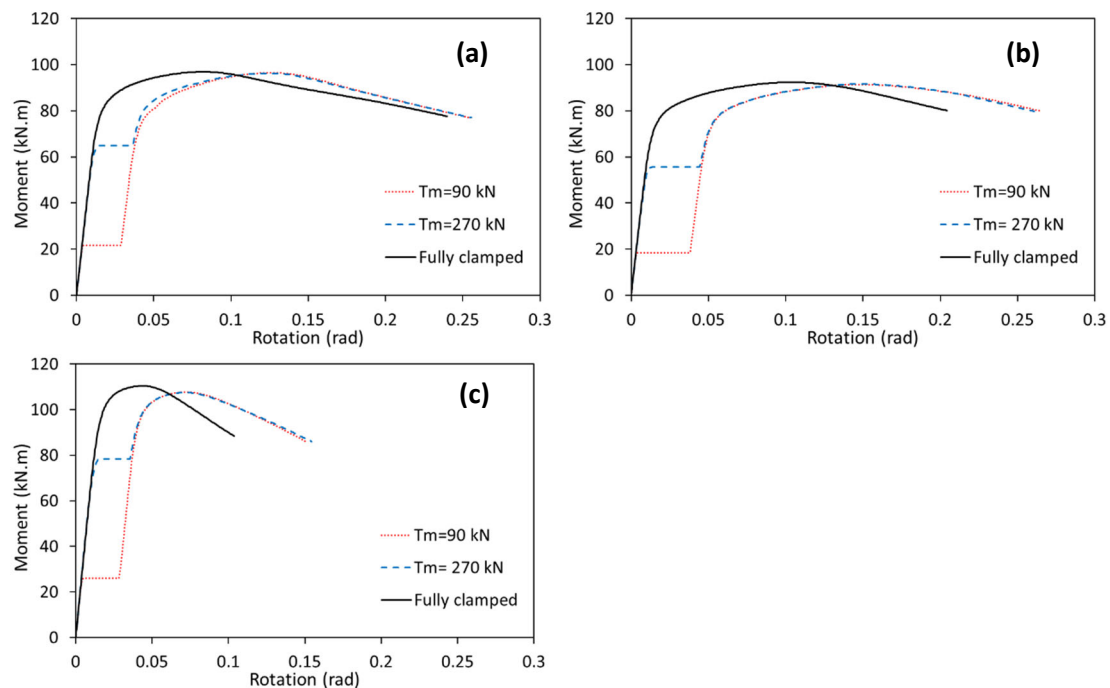
Fig. 16: The behaviour of connection with cross section class 1 using different bolt pretension forces and configurations: (a) Circle, (b) Diamond, (c) Square

5. Efficiency of CFS bolted moment connections with friction-slip fusing mechanism

In this section, the results of the comprehensive parametric study are used to identify the most efficient design solutions for CFS bolted moment connections with friction-slip fusing mechanism using different response parameters.

5.1 Moment-rotation behaviour

In this section, the flat-flange channels with various thicknesses (1, 2, 4 and 6 mm) and circle distribution of the bolts is selected to show the typical cyclic response of the connections mobilised with friction-slip fusing system (Fig. 17). The cyclic moment-rotation envelope is specified in both positive and negative rotations by plotting the locus of peak moment points at the first cycle of each load amplitude. It should be noted that, unlike the monotonic moment rotation backbone curve, the cyclic moment-rotation envelope can take into account the strength degradation due to cyclic loading as observed in the previous experimental tests on CFS elements and connections [29, 32, 33]. The rotation of the connection was quantified as the ratio of beam tip displacement to the length of the beam up to the gusset plate. In the following sections, the moment-rotation results are used to determine different performance parameters such as moment capacity, energy dissipation, equivalent viscous damping coefficient, and ductility ratio. It is worth mentioning that the dominant mode of failure in the selected connections with and without friction-slip is always local buckling in the CFS beam. However, the deformation of buckled area of the beam is less intensified when slip action is activated in the connection (see Fig. 10).
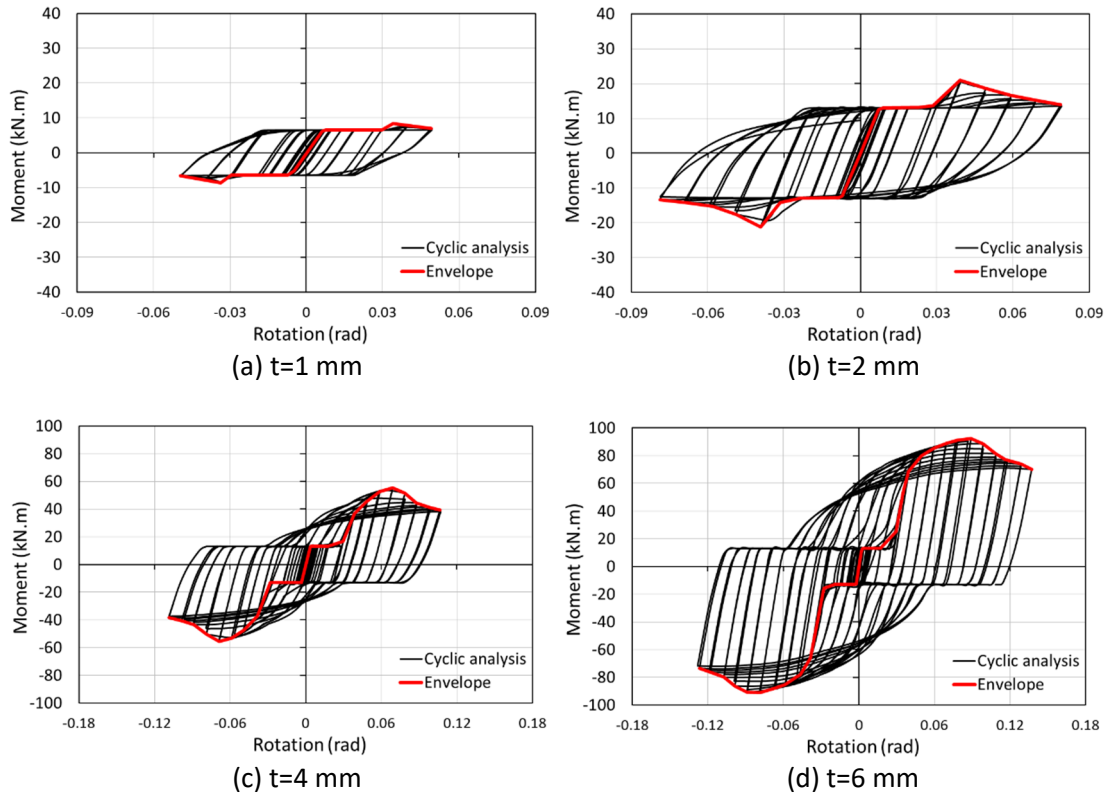
Fig. 17: Moment-rotation cyclic relationship and envelope curve of the connections with flat-flange beam section and circular bolt arrangement

5.2 Moment capacity of the connections

Fig. 18 shows the maximum moment capacity of both connections with and without bolting friction-slip fuse, indicating the effect of bolt slippage is generally negligible on the flexural capacity of the connections regardless of the beam cross-sectional class. The minor differences can be attributed to the fact that after bolt slippage the centre of rotation shifts from the centre of the bolts, leading to a small change in the maximum flexural capacity of the connections. As shown in Fig. 18, the cross-sectional class of the CFS beam elements and the arrangement of the bolts seem to be the most important design parameters affecting the capacity of the connections. In general, using a square bolt arrangement leads to a higher bending moment capacity especially in the case of CFS beam elements with class 1 and 2 (6 mm and 4 mm), where up to 32% increase is observed compared to the other bolt arrangements. While it was previously shown that bent flange sections can provide noticeably higher moment capacity compared to standard flat-flange sections [10, 34], the

results of this study indicate that using bent flange sections can increase the capacity of the connections by less than 10%. This is referred to two main reasons: (i) effect of bi-moment generated due to presence of bolts [8], and (ii) using channels with deep web generally reduces the effects of the flange on the moment capacity of the connections.

Fig. 18: Moment capacity of CFS connections as a function of bolt configuration and cross-section class (C1, C2, C3, and C4 are cross-section classes 1, 2, 3 and 4, respectively)

5.3 FEMA bi-linear idealisation model

To characterize the cyclic behaviour of the CFS bolted moment connections, the idealised bi-linear models recommended by FEMA-356 [35] are developed based on the cyclic moment-rotation envelopes (see Section 5.1). As shown in Fig. 19, the FEMA proposed models use an ideal bilinear elastic plastic curve to represent the non-linear behaviour of an assembly by incorporating an energy balance approach. The yield rotation (θ_y) is determined on the condition that the secant slope intersects the actual envelope curve at 60% of the nominal yield moment (M_y), while the area enclosed by the bilinear curve is equal to that enclosed by the original curve bounded by the target displacement (θ_t). The adopted model